Power Electronic Systems
Laboratory

Proceedings of the 16th European Conference on Power Electronics and Applications (EPE 2014 - ECCE Europe), Lappeenranta, Finland, August 26-28, 2014

Impact of PV String Shading Conditions on Panel Voltage Equalizing Converters and Optimization of a Single Converter System with Overcurrent Protection

M. Kasper,
S. Herden,
D. Bortis,
J. W. Kolar

Eidgenössische Technische Hochschule Zürich
Swiss Federal Institute of Technology Zurich

Impact of PV String Shading Conditions on Panel Voltage Equalizing Converters and Optimization of a Single Converter System with Overcurrent Protection

Matthias Kasper, Stefan Herden, Dominik Bortis and Johann W. Kolar
Power Electronic Systems Laboratory
ETH Zurich, Physikstrasse 3
Zurich, 8092, Switzerland
kasper@lem.ee.ethz.ch

Keywords

<<Photovoltaic>>, <<ZVS converters>>, <<Renewable energy systems>>, <<Fault handling strategy>>, <<Passive component integration>>.

Abstract

Unequal irradiance of series connected PV panels in a string strongly decreases the output power of the PV system, as either PV panels are bypassed or operated below their MPP. By connecting balancing converters around each pair of adjacent PV panels, all panels can maintain the operation close to their MPP regardless of any mismatched operating condition. In this paper a balancing converter concept with ZVS is introduced and the operation of a string of PV panels equipped with balancing converters is analytically described. Based on this analytic framework, different examples of shading scenarios of a PV string are examined regarding the average inductor current values that occur within the balancing modules, in order to derive the required specifications of a balancing converter. Moreover, a two-level overcurrent protection concept is introduced which enables to keep all balancing converters within the safe operating area at all times, even at shading conditions with high mismatch. Furthermore, the design optimization of a highly efficient PV voltage balancing converter with a wide input voltage range is explained in detail and finally the concept is verified with measurement results of a demonstrator system.

1 Introduction

In today's grid-connected photovoltaic (PV) energy systems several PV panels are connected in series to form strings in order to reach a bus voltage which is suitable for a central inverter to feed power into the grid. The series connection of PV panels implies that all PV panels within a string conduct the same current. Since the generated photocurrent of a PV panel is mainly proportional to the received irradiance, however, mismatched operating conditions within a PV string lead to different current levels and thus violate the premise of series connected sources. As a measure to prevent the creation of hotspots in panels with lower current generation and the resulting destruction of the panel, usually diodes are placed in anti-parallel to the strings of PV cells of a panel. These bypass diodes are biased in forward direction if the string current exceeds the level of the short circuit current of the panel and the bypass diode conducts the excess current. Thus, with mismatched operating conditions such as e.g. caused by partial shading, dust or debris on the panels or due to unequal aging processes, the output power of a PV string is decreased since either the power of shaded panels is lost or, if the level of the string current is decreased, the output power of the unshaded panels is below their maximum power point (MPP).

The impact of mismatched operating points on the total output power of a string can be limited by the application of DC-DC converters on PV panel level. Different converter concepts have been proposed in literature, which can be divided into series and parallel connected concepts with sub-categories of full and partial-power converters [1]. The partial-power concepts are likely to feature a higher conversion

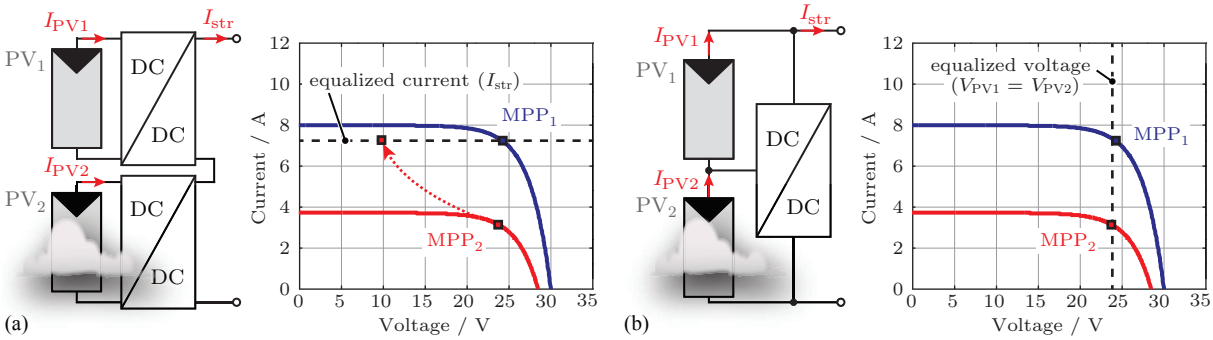

Figure 1: Comparison of different PV panel integrated DC-DC converter concepts (cf. [1]) for a simplified system with two PV panels receiving different levels of irradiance: (a) the series connected full-power converter concept adjusts the maximum power points MPP_1 and MPP_2 of the PV panels to a common string current I_{str}. (b) The analyzed parallel connected partial-power concept equalizes all PV panel voltages such that the panel voltages are equal or close to the MPP voltages.

efficiency and a smaller converter volume as only a fraction of the full PV panel power has to be processed by the converter. Therefore, especially the parallel connected partial-power converter (P-PPC) has been the focus of several research papers [2–12]. Many of these topologies have been known for more than two decades from battery equalization circuits, where the state of charge of series connected battery cells is equalized in order to prevent unequal aging of the batteries [2, 3]. However, this "virtual parallel" connection of battery cells cannot only be used for battery systems or auxiliary supplies with high conversion ratios [4] but can also be applied to PV panels [5–7] or on sub-string level to strings of PV cells [8–12].

In contrast to previous papers, which mainly focus either on the theoretical analysis of different balancing topologies or on advanced control schemes, this paper provides an analytical background of both the operation of the proposed converter concept and the operation of the whole PV system, as presented in Sections 2 and 3. A novel contribution of this paper is hereby the analysis of different shading scenarios of a PV string on the operating points of the balancing converters. Section 4 introduces the two-level overcurrent protection concept and the adjustment of the operating points of each balancing converter of a PV string installation if an overcurrent exceeds the safe operating limits. This constitutes the basis for a converter optimization as described in Section 5. Based on those results, a set of converter prototypes are designed, built up and tested in string operation with different shading scenarios, as shown in Section 6. The final Section 7 contains the conclusion of PV panel voltage equalizing converters.

2 Operating Principle

In this section the fundamental operating principle of balancing converters in PV systems and the topology of the proposed converter are explained. In order to extract the maximum amount of power from a string of PV panels, each PV panel has to be operated at its maximum power point (MPP). On the one hand, this can be achieved with full-power DC-DC converters on each PV panel that adjust the PV panel current I_{PV} to the string current I_{str}, as shown in **Fig. 1(a)**. Those converters can either be buck, boost or buck-boost converters. On the other hand, instead of adjusting all PV panels to the same current, they can also be operated with the same panel voltage by means of partial-power balancing and/or panel voltage equalization converters, since the voltage of the MPP of a panel is barely affected by the level of received irradiance, as visualized in **Fig. 1(b)**. In contrast to full-power converters, however, the partial-power balancing converters cannot track the MPPs of the PV panels; the overall MPP tracking of the whole string in this case is performed by the central inverter. Furthermore, due to the series connection of the PV panels in the balancing converter concept, the voltage of the string is given by the addition of the individual PV panel voltages. Thus, paralleling multiple strings is only feasible if all strings contain the same number of PV panels. Those limitations regarding the flexibility of the system design, however, are in many cases outweighed by a lower complexity and higher efficiency of the balancing converters, since they convert only a small part of the panel power, defined by the differences of the actual PV panel current values.

The balancing converters denoted as B_1, B_2 in **Fig. 2(a)**, are inverting buck-boost DC-DC converters,

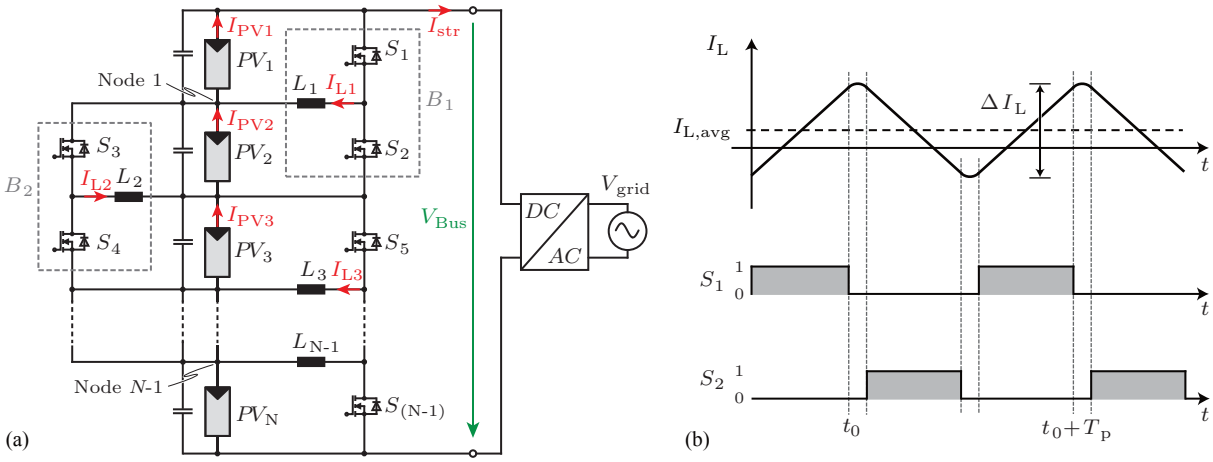

Figure 2: Analyzed PV system with balancing circuits: (a) circuit diagram showing a PV string with N PV panels (PV_1,...,PV_N), $N-1$ balancing converters (B_1,...,$B_{(N-1)}$) and a grid connected DC-AC inverter and (b) characteristic inductor current waveform and gate signals of one balancing module.

each connected around two adjacent PV panels. This means, that a PV string consisting of N PV panels requires $(N-1)$ balancing converters, i.e. $(2\cdot(N-1))$ switches and $(N-1)$ inductive components in total.

The balancing converters do not require any closed loop control since the switches of each buck-boost converter can be controlled by a simple PWM signal with a fixed duty cycle of 50% in case of normal operation without over-current. Furthermore, the balancing converters operate independently of each other and neither require any communication or synchronization with neighboring converters nor with the central inverter.

The waveform of the gate signals and the inductor current are shown in **Fig. 2(b)** for one balancing converter. The triangular current of the inductor can be utilized in combination with the parasitic drain-source capacitances of the MOSFETs to achieve zero-voltage switching (ZVS), as the current direction reverses during each conduction interval. In order to maintain ZVS operation over the whole PV panel voltage range, the switching frequency is linearly adjusted with the PV panel voltage by means of a voltage controlled oscillator (VCO). This results in a constant peak-to-peak current ripple ΔI_L of the inductor current I_L.

2.1 Panel Level vs. Sub-String Level Equalization

In recent publications a voltage equalization on sub-string level of the PV panels has been proposed [8–12]. This is motivated by the fact that a PV panel usually consists of two or three strings of series connected PV cells, so-called sub-strings. They are equipped with bypass diodes, as depicted in **Fig. 3(a)** for a PV panel with two sub-strings. Thus, if equalization modules are connected around the sub-strings, each sub-string can be operated at its MPP. In contrast, the equalization on PV panel level, however, only regulates the terminal voltage of the PV panel and not the voltages of the sub-strings. The current through the sub-strings is equal to the PV panel current which is drawn from the terminals of the PV panel. The whole system, consisting of the PV panels with balancing converters and the central DC-AC inverter, is driven by the MPP tracker of the central inverter to strive for maximum output power. The current within the PV panels will adjust to the value that still yields the required PV panel voltage which is the voltage applied to the PV panel by the balancing converters.

As a result, in a partially shaded PV panel, the output power of the unshaded sub-strings will be below their MPP, since the shaded sub-string dictates the current level. This is visualized in **Fig. 3(b)** for a PV string with two PV panels and one balancing converter, where the upper panel is unshaded and the lower panel is partially shaded. The panel voltage V_{PV2} is equal to the voltage of the upper PV panel V_{PV1} as a result of the equalization process. The current I_{PV2} of the partially shaded panel is therefore given by the intersection of the PV panel terminal characteristics and the impressed voltage V_{PV2}.

In practice, however, only few PV panels, namely these at the border of shaded and unshaded areas, will be partially shaded. Thus, the benefit of sub-string level equalization circuits compared to panel level balancing converters is in most cases outweighed by higher system costs resulting from the increased part count.

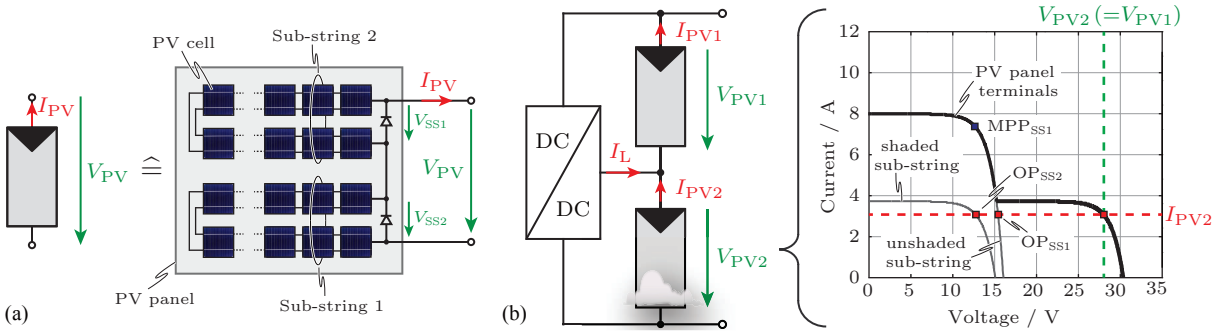

Figure 3: Issue of partial shading of a PV panel: (a) structure of a standard crystalline Silicon PV panel with two internal strings (i.e. sub-strings) of PV cells with bypass diodes; (b) simplified system with a voltage balancer around an unshaded PV panel (PV panel 1) and a partially shaded PV panel (PV panel 2) and the corresponding current/voltage diagram of the partially shaded PV panel with the operating points of the unshaded and shaded sub-string, OP_{SS1} and OP_{SS2}, respectively.

3 Analytical Description

In this section the operation of a PV string with balancing converters is analytically described in order to determine the influence of different shading conditions on the operation of the converters. In case of any mismatch between the PV panels within a string, the currents in the inductors of the balancing converters exhibit DC values $I_{L1},...,I_{L(N-1)}$ (cf. **Fig. 2(a)**). The values of these DC currents can be calculated depending on the values of the PV panel currents ($I_{PV1},...,I_{PV(N)}$) as long as a duty cycle of 50% is maintained and also due to the fact that no DC current can flow through the capacitors. The current direction is inherited from **Fig. 2(a)** and, based on Kirchoff's current law, the equations for the $(N-1)$ nodes between each pair of adjacent PV panels can be written as

$$\begin{aligned}
&\text{Node 1:} && I_{PV2} - I_{PV1} + I_{L1} - \frac{1}{2}\cdot I_{L2} = 0 \\
&\text{Node 2:} && I_{PV3} - I_{PV2} + I_{L2} - \frac{1}{2}\cdot I_{L1} - \frac{1}{2}\cdot I_{L3} = 0 \\
& && \vdots \\
&\text{Node N-2:} && I_{PV(N-1)} - I_{PV(N-2)} + I_{L(N-2)} - \frac{1}{2}\cdot I_{L(N)} - \frac{1}{2}\cdot I_{L(N-3)} = 0 \\
&\text{Node N-1:} && I_{PV(N)} - I_{PV(N-1)} + I_{L(N-1)} - \frac{1}{2}\cdot I_{L(N-2)} = 0\,.
\end{aligned} \tag{1}$$

This can also be expressed in matrix form as

$$\begin{bmatrix}
1 & -\frac{1}{2} & 0 & & \cdots & 0 & 0 \\
-\frac{1}{2} & 1 & -\frac{1}{2} & 0 & & & 0 \\
0 & -\frac{1}{2} & 1 & -\frac{1}{2} & 0 & & \vdots \\
 & \ddots & \ddots & \ddots & \ddots & \ddots & \\
\vdots & & 0 & -\frac{1}{2} & 1 & -\frac{1}{2} & 0 \\
0 & & & 0 & -\frac{1}{2} & 1 & -\frac{1}{2} \\
0 & 0 & \cdots & & 0 & -\frac{1}{2} & 1
\end{bmatrix} \times \begin{bmatrix} I_{L1} \\ I_{L2} \\ I_{L3} \\ \vdots \\ I_{L(N-1)} \end{bmatrix} = \begin{bmatrix} I_{PV2} - I_{PV1} \\ I_{PV3} - I_{PV2} \\ I_{PV4} - I_{PV3} \\ \vdots \\ I_{PV(N)} - I_{PV(N-1)} \end{bmatrix} \tag{2}$$

By applying mathematical reformulation, the average inductor current $I_{L,n}$ of one balancing converter can be expressed in a summation of the PV panel currents as

$$I_{L,n} = 2\cdot\left(\sum_{i=1}^{n}\frac{N-n}{N}\cdot I_{PV,i} - \sum_{i=n+1}^{N}\frac{n}{N}\cdot I_{PV,i}\right)\,. \tag{3}$$

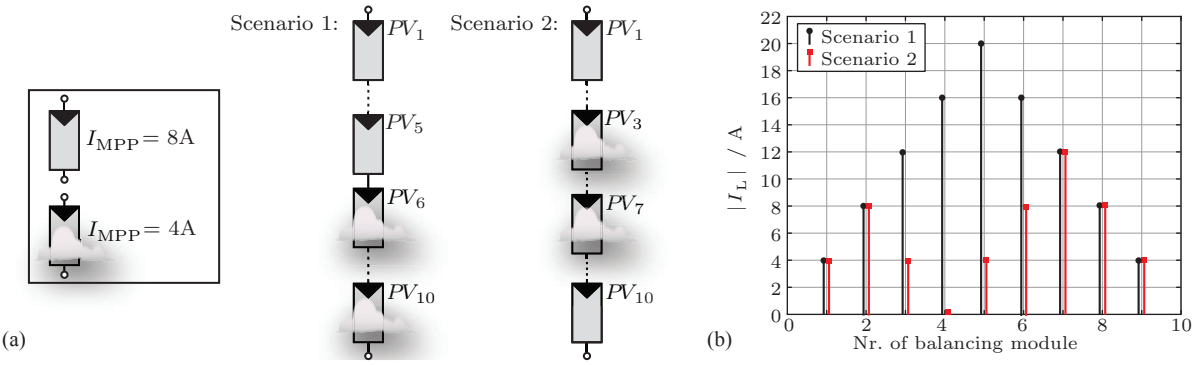

Figure 4: Impact of different shading scenarios on average current values of inductors in balancing converters: (a) PV string with N = 10 PV panels and two different shading scenarios. In both scenarios the same number of panels are shaded, but the shaded panels are located at different positions within the PV string: In scenario 1 the shaded panels are placed at the bottom of the string, whereas in scenario 2 the shaded panels are placed at the center of the string. (b) Average inductor current values I_L of balancing modules for both scenarios.

The DC string current I_{str}, that is drawn by the central inverter, can be calculated as

$$I_{str} = \frac{\sum_{i=1}^{N} I_{PV,i}}{N} \,. \tag{4}$$

Based on the DC string current I_{str}, the DC currents in the inductors (cf. (3)) can be expressed by a simple equation in only one summation as

$$I_{L,n} = 2 \cdot \left(\sum_{i=1}^{n} \Delta I_i \right) \tag{5}$$

where $\Delta I_i = I_{PV,i} - I_{str}$ is the difference between the PV panel current and the string current. Based on (3), the average value of the inductor current in each balancing module can be calculated for different shading scenarios. In **Fig. 4** two shading scenarios are depicted for a string with 10 PV panels and 9 balancing modules. In both scenarios the same numbers of shaded and unshaded panels is assumed (i.e. 4 shaded and 6 unshaded panels). Furthermore, it is assumed that all panels are operated at their MPP where the unshaded panels deliver $I_{MPP,unsh} = 8\,A$ and the shaded panels provide $I_{MPP,sh} = 4\,A$. In scenario 1 the shaded panels are placed at the end of the string whereas in scenario 2 the shaded panels are located at the center of the string. The resulting average inductor current values in each balancing module are visualized for both scenarios in **Fig. 4(b)**. The largest average value that appears in scenario 1 amounts to $I_{L,max} = 20\,A$ whereas the largest value in scenario 2 is only $I_{L,max} = 12\,A$ and thus only 60% the value of scenario 1. This aspect has not been discussed in the literature so far and constitutes an important point in the course of the converter design and selection of a proper protection concept in order to prevent overloading of balancing converters in a PV system in certain shading situations.
The most critical operation in matters of shading situations of a PV panel string is a two-part distribution of the shaded and the unshaded PV panels, given that there is then just one balancing module in the total string with an adjacent shaded and unshaded PV panel. Then, the DC inductor current of this balancing module carries the maximum DC inductor current. For an analytical derivation of the maximum DC value of the inductor current the DC string current I_{str} is expressed in dependency on the amount of shaded PV panels n, a ratio of irradiance k_{irr}, and the PV panel current I_{PV} of unshaded panels in their MPP.

$$I_{str} = \frac{I_{PV} \cdot (N-n) + k_{irr} \cdot I_{PV} \cdot n}{N} \tag{6}$$

Inserting (6) in (5) and differentiating with respect to n yields a maximum DC inductor current at $n = \frac{N}{2}$ which equals

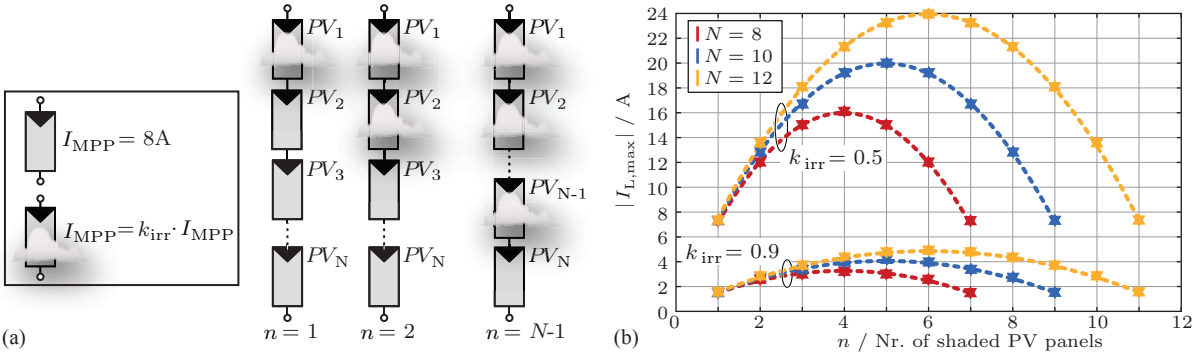

Figure 5: The maximum DC inductor current that occurs in the balancing converter with an adjacent shaded and unshaded PV panel for shading scenarios where the string is divided into a shaded and an unshaded section. The DC inductor current of this balancing module gets higher when, 1) the string gets longer, 2) the amount of shaded and unshaded PV panels is balanced, and 3) the ratio of irradiance k_{irr} decreases.

$$I_{L,max}\left(n = \frac{N}{2}\right) = \frac{1}{2} \cdot (1 - k_{irr}) \cdot N \cdot I_{PV} \,. \tag{7}$$

Based on (5) the maximum DC inductor currents for n shaded PV panels are illustrated in **Fig. 5** where the combination of $k_{irr} = 0.5$, $N = 10$ and $n = 5$ corresponds to scenario 1 of **Fig. 4**.

The DC current of an inductor also influences the RMS current values in the switches of a balancing module and thus the conduction losses. The RMS current value of a switch can be expressed as a function of the peak-to-peak inductor current ripple ΔI_L and of the average inductor current I_L, by

$$I_{sw,rms} = \frac{1}{2}\sqrt{2 \cdot I_L^2 + \frac{1}{6}\Delta I_L^2} \,. \tag{8}$$

Furthermore, the efficiency of a PV system with N PV panels and $N-1$ the balancing converters can be calculated by taking into account the power generated by the PV panels ($P_{PV,1}, \ldots, P_{PV,N}$) and the losses in the balancing converters ($P_{Loss,1}, \ldots, P_{Loss,N\text{-}1}$), which results in

$$\eta_{Sys} = \frac{\sum_{i=1}^{N} P_{PV,i} - \sum_{i=1}^{N-1} P_{Loss,i}}{\sum_{i=1}^{N} P_{PV,i}} \,. \tag{9}$$

4 Over-Current Protection

The currents in the balancing modules might exceed the limit of the safe operating area as a result of unfavorable shading scenarios, meaning the balancing module drops out of ZVS due to a large DC current. This might lead to either the saturation of the inductor and/or to the thermal destruction of the MOSFETs caused by the switching losses. Therefore, a two-level protection concept is used in order to counteract high DC inductor current values and guarantee safe operation. In a first step the balancing modules is kept in the safe operating area by adjusting the duty cycle within a balancing module. In a second step, in case a situation with very fast changes of the operating points of the PV panels occurs, the balancing module is bypassed by turning off the MOSFETs. The protection methods are described in more detail in the following paragraphs.

The balancing module loses ZVS when the DC value of the inductor current exceeds half of the peak-to-peak inductor current ΔI_L. Thus, the duty cycle adjustment is initiated as soon as the measured DC value of the inductor current exceeds a predefined value. The direction of the duty cycle adjustment is given by the sign of the DC current. The duty cycle is changed until the DC current is below the limit. This allows to operate the PV panels in operating points with different voltages and therefore smaller differences in

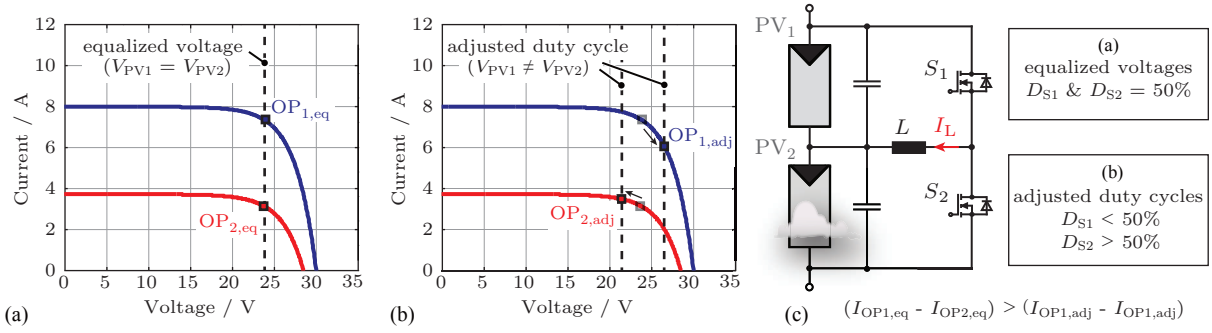

Figure 6: Operating points of (a) two PV panels with equalized voltages and (b) unequalized voltages due to duty cycle adjustment. The duty cycle adjustment keeps the balancing converter in the safe operating area with ZVS since the DC inductor current I_L is decreased by the adjustment.

the PV currents, as shown in **Fig. 6**. As a drawback of this protection measure, however, the PV panels are moved out of their MPP and operate in a sub-optimal operating point. Since the shading situation might change over time, the controller tries to bring back the duty cycle ratio to the initial value of 50 %.

In case the duty cycle modification cannot provide safe operation and the DC inductor current exceeds a defined limit, the second level of the protection concept is activated and the balancing module is turned off. By turning off a balancing module, the string of PV panels is divided into two parts that are internally balanced by the remaining converters. Thus, the string contains two MPPs and the central inverter tracks the MPP with the highest power. A restart of the turned-off balancing module can be attempted once the voltages of the adjacent panels are in close vicinity.

5 Balancing Converter Optimization and Realization

In this section the optimization procedure and design of the prototype are explained. The balancing converter specifications do not only depend on the electrical characteristics of the PV panels but also on the expected shading scenarios i.e. the difference between the generated panel currents within a string. Since worst case scenarios can result in high average inductor current values, as described and depicted in chapter 3, the design of the converter has to be limited to reasonable shading scenarios. With larger values of the maximum average inductor current, the balancing converter can work in a wider range of shading conditions without reaching the limits at which the protection circuits are activated. This, however, leads to larger constant losses due to the larger peak-to-peak current ripple in the inductor and larger RMS current values in the MOSFETs. Thus, as a result of this trade-off, the maximum average inductor current up to which the switches can operate in ZVS is set to $I_{L,max} = 5\,A$. In order to achieve ZVS the amplitude of the peak-to-peak inductor current ripple ΔI_L has to be twice the maximum average inductor current $I_{L,max}$, i.e. $\Delta I_L = 10\,A$. The switching frequency is linearly adjusted to the PV panel voltage by a voltage controlled oscillator (VCO) that senses the voltage across both PV panels. This yields a constant volt-second $\lambda_L = V_{PV}/(2 \cdot f_{sw})$ which is applied across the main inductor of a balancing

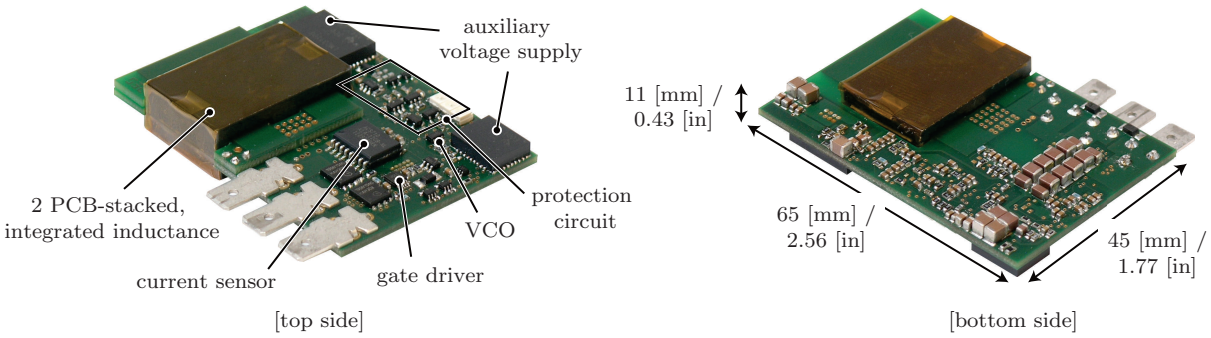

Figure 7: Dimensions and components of the voltage balancing converter prototype for PV panel voltages of $V_{PV} = 16\,V...50\,V$.

Table I: List of main components per balancing converter.

Component	**Specifications**
2x MOSFETs	BSC190N15NS3 / Infineon [$R_{DS,on} = 19\,m\Omega$ @ $T_j = 25\,°C$, $V_{DS} = 150\,V$, $I_D = 50\,A$]
1x Gate driver	Half-bridge gate driver LM5106 / Texas Instruments
1x PCB integrated Inductor	ELP32/6/20, N87 ferrite / EPCOS [$L \approx 9.5\,\mu H$, 6 turns, 2 stacked 4-layer PCBs, track width $t_w \approx 7\,mm$, copper thickness $t_h = 35\,\mu m$, $l_{airgap} = 0.37\,mm$]
1x VCO	LTC6992-2 / Linear Technology
2x Auxiliary supply	LMZ35003 & LMZ31503 / Texas Instruments
2x Capacitors	X7R ceramic capacitors [$C = 10.8\,\mu F$ (4x2.2 µF and 2x1.0 µF), $V_{rated} = 100\,V$]

module during a switching state and thus, also yields a constant inductor current ripple ΔI_L for all PV panel voltages. Hence, the inductance of the main inductor can be expressed as $L = \lambda_L/\Delta I_L$.

The PV panel voltage is strongly influenced by the PV panel temperature, thus the converter has to be designed for a wide input voltage range, i.e. $V_{PV} = 16\,V...50\,V$ covering a factor of $k = V_{PV,max}/V_{PV,min} = 3.125$. The switching frequency has to be varied with the same factor between maximum and minimum switching frequency. Since half-bridge gate drivers usually have a fixed dead-time (often in the range of around $T_{dead} = 100 - 200\,ns$), the maximum switching frequency is chosen to be $f_{max} = 250\,kHz$, so that the total dead-time is less than 10% of the total switching period. As a result, the prototype operates with a switching frequency in the range of $f_{sw} = 80\,kHz...250\,kHz$ which translates into $\lambda_L = 100\,\mu Vs$ and a required inductance of $L = 10\,\mu H$.

In order to achieve a compact converter layout with minimal height to facilitate the integration into the junction box of a PV panel, a PCB integrated inductor design has been chosen. Thus, for the optimization of the inductor all available EPCOS N87 cores with ELP and I-core shape for PCB-integration have been considered. The losses in the inductor can be divided into core losses and winding losses. For the calculation of the core losses the improved generalized Steinmetz equation (iGSE) has been applied. The eddy current losses in the PCB tracks of the integrated inductor have been calculated based on the results of [13]. The combined core and winding losses of the chosen inductor design (cf. **Table I**) amount to 1.93 W at PV panel voltages of 25 V. The conduction losses in the MOSFETs at a junction temperature of $T_j = 25\,°C$ are calculated as $P_{MOSFET,cond} = 180\,mW$ based on (8).

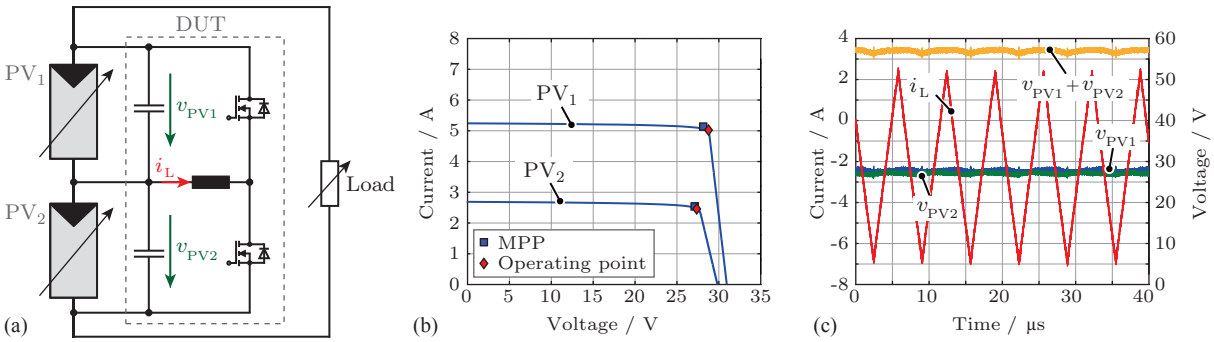

Figure 8: Voltage balancing converter measurement setup and results: (a) measurement setup where a SAS is used to emulate two PV panels and an electronic load to emulate the central inverter; (b) parameters of the emulated PV panels (PV_1 and PV_2) and measured operating points; (c) measured waveforms of the inductor current i_L and PV panel voltages v_{PV1} and v_{PV2}.

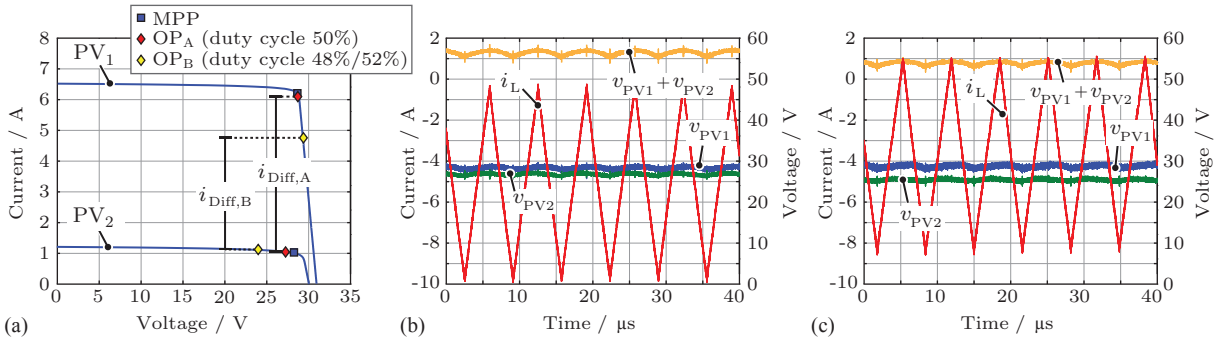

Figure 9: Measurement results of the overcurrent protection concept: (a) operating points OP_A and OP_B of a system consisting of one heavily shaded and one unshaded PV panels with a balancing converter for the cases without any protection concept (i.e OP_A) and with the proposed protection concept (i.e OP_A); (b) measured voltage and current waveforms for the operation without any protective measures with the MOSFETs operating at hard switching; (c) activated protection concept where the PV panels are operated at different voltages with a smaller current difference and thus the triangular current is utilized for ZVS.

6 Measurement Results

The measurement setup and results of one balancing converter connected around two PV panels are shown in **Fig. 8**. The electrical characteristics of PV panels were emulated with a Solar Array Simulator (SAS) by Agilent (E4360) and the central DC-AC inverter was resembled by an electronic load (Chroma / 63200) which was operated in constant voltage mode. The applied test scenario reflects the case of one unshaded PV panel with a maximum output power of $P_{PV1,MPP} = 145\,W$ (i.e. $V_{PV1,MPP} = 29\,V$ and $I_{PV1,MPP} = 5\,A$) and a shaded panel with a maximum output power of only $P_{PV2,MPP} = 70\,W$ (i.e. $V_{PV2,MPP} = 28\,V$ and $I_{PV2,MPP} = 2.5\,A$). With the application of the balancing module, both PV panels can be operated in or close to their MPP as visible in **Fig. 8(b)**. The measured inductor current waveform with triangular shape and the balanced PV panel voltages are depicted in **Fig. 8(c)**.
The protection circuitry was tested with a scenario where one panel is unshaded (i.e. $P_{PV1,MPP} = 145\,W$, $V_{PV1,MPP} = 29\,V$ and $I_{PV1,MPP} = 6.5\,A$) and the second panel is heavily shaded (i.e. $P_{PV2,MPP} = 28\,W$, $V_{PV2,MPP} = 28\,V$ and $I_{PV2,MPP} = 1.0\,A$) with only a fraction of the power of the unshaded panel. Without any protective measures, the average inductor in the balancing module is driven above the predefined upper limit of 5 A and the MOSFETs are operated in hard switching mode since there is no change in the direction of the current anymore, as shown in **Fig. 9(b)**. When the protection circuit is active, however, the duty cycles of the balancing converter are slightly adapted until they reach 48 % / 52 %. This allows to drive the operating points of the PV panels to values with a lower current difference, i.e. the unshaded PV panel is operated at a voltage above the MPP whereas the shaded PV panel is operated at a voltage below its MPP. Then the absolute value of the average current in the inductor decreases and, since the current changes its direction at each switching state, the MOSFETs are operated with ZVS, as depicted in **Fig. 9**.

The total losses in one balancing module at no load operation (i.e. no mismatch between the PV panels) for PV panel voltages of 25 V were measured to be $P_{Loss,tot} = 2.65\,W$, where the losses that can be attributed to the auxiliary electronics account for around $P_{Loss,aux} \approx 550\,mW$. As a result, in a PV system with a string of 10 equally irradiated PV panels with an output power of $P_{MPP} = 220\,W$ each, the system efficiency reaches $\eta_{Sys} = 99.0\%$ based on (9).

7 Conclusions

In this paper, a voltage balancing converter for PV panel integration with a high efficiency, low part count, small size and easy controllability has been presented. The converter is designed to operate with ZVS at all operating points by adjusting the switching frequency depending on the PV panel voltage and by an additional two-level overcurrent protection concept. The two-level protection concept still provides safe operation with ZVS at undesired shading scenarios due to the adjustment of the duty cycle, otherwise a balancing module shut down is initiated for protection reasons. Furthermore, an analytical framework has been introduced to describe the current distribution within a PV system with an arbitrary number

of PV panels and corresponding balancing converters. Based on this analytic framework a converter optimization has been performed and a compact prototype has been assembled. The measurement results show that the output power of a string with PV panels receiving different irradiance can be maximized with a very high efficiency. The protection concept is verified with measurements at two very unequally irradiated PV panels.

References

[1] M. Kasper, D. Bortis, and J. Kolar, "Classification and Comparative Evaluation of PV Panel-Integrated DC–DC Converter Concepts," *IEEE Trans. Power Electron.*, vol. 29, no. 5, pp. 2511–2526, 2014.

[2] N. H. Kutkut, "A Modular Nondissipative Current Diverter for EV Battery Charge Equalization," in *Proc. of the 13th Annual Applied Power Electronics Conf and Exposition (APEC)*, vol. 2, pp. 686–690, 1998.

[3] Schmidt and C. Siedle, "The Charge Equalizer - A New System to Extend Battery Lifetime in Photovoltaic Systems, UPS and Electric Vehicles," in *Proc. of the 15th International Telecommunications Energy Conference (INTELEC)*, vol. 2, pp. 146–151, 1993.

[4] M. Kasper, D. Bortis, and J. W. Kolar, "Novel High Voltage Conversion Ratio "Rainstick" DC/DC Converters," in *Proc. of the Energy Conversion Congress and Exposition (ECCE) USA*, pp. 789–796, 2013.

[5] G. R. Walker and J. C. Pierce, "PhotoVoltaic DC-DC Module Integrated Converter for Novel Cascaded and Bypass Grid Connection Topologies — Design and Optimisation," in *Proc. of the 37th IEEE Power Electronics Specialists Conf. PESC '06*, pp. 1–7, 2006.

[6] P. S. Shenoy, K. A. Kim, B. B. Johnson, and P. T. Krein, "Differential Power Processing for Increased Energy Production and Reliability of Photovoltaic Systems," *IEEE Trans. Power Electron.*, vol. 28, no. 6, pp. 2968–2979, 2013.

[7] D. Shmilovitz and Y. Levron, "Distributed Maximum Power Point Tracking in Photovoltaic Systems–Emerging Architectures and Control Methods," *AUTOMATIKA: časopis za automatiku, mjerenje, elektroniku, računarstvo i komunikacije*, vol. 53, no. 2, pp. 142–155, 2012.

[8] H. J. Bergveld, D. Büthker, C. Castello, T. Doorn, A. de Jong, R. van Otten, and K. de Waal, "Module-Level DC/DC Conversion for Photovoltaic Systems: The Delta-Conversion Concept," *IEEE Trans. Power Electron.*, vol. 28, no. 4, pp. 2005–2013, 2013.

[9] Kadri, J.-P. Gaubert, and G. Champenois, "Nondissipative String Current Diverter for Solving the Cascaded DC–DC Converter Connection Problem in Photovoltaic Power Generation System," *IEEE Trans. Power Electron.*, vol. 27, no. 3, pp. 1249–1258, 2012.

[10] C. Schaef, K. Kesarwani, and J. T. Stauth, "A Coupled-Inductor Multi-Level Ladder Converter for Sub-Module PV Power Management," in *Proc. of the 28th Annual IEEE Applied Power Electronics Conf. and Exposition (APEC)*, pp. 732–737, 2013.

[11] J. T. Stauth, M. D. Seeman, and K. Kesarwani, "Resonant Switched-Capacitor Converters for Sub-module Distributed Photovoltaic Power Management," *IEEE Trans. Power Electron.*, vol. 28, no. 3, pp. 1189–1198, 2013.

[12] S. Qin, S. T. Cady, A. D. Dominguez-Garcia, and R. C. N. Pilawa-Podgurski, "A Distributed Approach to MPPT for PV Sub-Module Differential Power Processing," in *Proc. of the Energy Conversion Congress and Exposition (ECCE), USA*, pp. 2778–2785, 2013.

[13] I. Lope, C. Carretero, J. Acero, J. Burdio, and R. Alonso, "Practical Issues when Calculating AC Losses for Magnetic Devices in PCB Implementations," in *Proc. of the 27th Applied Power Electronics Conference and Exposition (APEC)*, pp. 1017–1022, 2012.